

# Reduction of SO(2) symmetry for spatially extended dynamical systems

Nazmi Burak Budanur,<sup>1</sup> Predrag Cvitanović,<sup>1</sup> Ruslan L. Davidchack,<sup>2</sup> and Evangelos Siminos<sup>3</sup>

<sup>1</sup> *Center for Nonlinear Science, School of Physics,  
Georgia Institute of Technology, Atlanta, GA 30332-0430*

<sup>2</sup> *Department of Mathematics, University of Leicester, Leicester LE1 7RH, UK*

<sup>3</sup> *Max-Planck Institute for the Physics of Complex Systems,  
Nöthnitzer Str. 38, D-01187 Dresden, Germany*

(Dated: December 6, 2024)

Spatially extended systems, such as Navier-Stokes equations, are often equivariant under continuous symmetry transformations, with each state of the flow having an infinite number of equivalent solutions obtained from it by a symmetry action, such as a translation or a rotation. ‘Symmetry reduction’ is a coordinate transformation which separates the state space into a lower-dimensional, symmetry-reduced state space, where every set of symmetry-equivalent states is represented by a single state, and ‘phase’ coordinates which enable one to reconstruct the original, full state space dynamics. In the method of slices this reduction is achieved locally by cutting all group orbits by a ‘slice’. Here we describe the ‘first Fourier mode slice’, a simple application of the method to reduction of SO(2) symmetry, in which singularities in phase velocity close to the slice border are regularized by a time-scaling transformation. We show that global structures, such as chaotic attractors and unstable manifolds of traveling waves, are uncovered in the symmetry-reduced state space. We illustrate the method by applying it to a two-Fourier modes normal-form model and to the Kuramoto-Sivashinsky system.

PACS numbers: 02.20.-a, 05.45.-a, 05.45.Jn, 47.27.ed

A solution to a problem in classical or quantum mechanics starts with the classification of problem’s symmetries, followed by a choice of a basis invariant under these symmetries. For example, one formulates the two-body problem in three Cartesian coordinates, but when it comes to solving it, polar coordinates, with the phase along the symmetry direction as an explicit coordinate, are preferable. While a classification of problem’s symmetries might be relatively straightforward, for high-dimensional nonlinear systems a good choice of a symmetry-invariant frame is not as easy as transforming to polar coordinates. The applications we have in mind are to solutions of spatially extended systems such as Navier-Stokes equations on a spatially periodic domain, where one starts the symmetry analysis by rewriting the equations in a Fourier basis,

$$u(x, \tau) = \sum_{k=-\infty}^{+\infty} \tilde{u}_k(\tau) e^{iq_k x}, \quad \tilde{u}_k = x_k + i y_k, \quad (1)$$

where  $q_k = 2\pi k/L$  and  $L$  is the domain size. Thus a nonlinear PDE is converted to an infinite tower of ODEs. In computations this state space is truncated to  $d = 2m$  real dimensions,  $a = (x_1, y_1, x_2, y_2, \dots, x_m, y_m)^T$ . (In examples considered here, Galilean invariance implies that 0-th Fourier mode can be set equal to zero.)

If the system has a translational symmetry, in choosing a Fourier basis we pick one particular reference basis from the continuous family of equivalent basis sets related by SO(2) rotations. In such a basis there is a redundant degree of freedom, namely the direction along which the problem is symmetric. Keeping such redundant degrees

of freedom not only makes a problem harder to solve, but, as we shall illustrate with our examples, also obscures its dynamics.

Symmetry reduction offers a systematic method of finding the coherent structures believed [1] to play an important role in shaping the state space of turbulent flows and illuminating their relations. Here we describe the ‘first Fourier mode slice’, a straightforward implementation of the method of slices [2–7] that can be used to reduce the SO(2)-symmetry in spatially extended systems. Consider a first-order dynamical system  $\dot{a} = v(a)$  defined on state space  $a \in \mathcal{M}$ ,  $v(a) = (\dot{x}_1, \dot{y}_1, \dot{x}_2, \dot{y}_2, \dots, \dot{x}_m, \dot{y}_m)$ . We assume that the equations of motion and the boundary conditions are invariant under an SO(2) group of transformations, i.e., that the dynamics satisfies the equivariance condition

$$v(a) = g^{-1}v(ga), \quad (2)$$

where

$$g(\theta) = \text{diag} [ R(\theta), R(2\theta), \dots, R(m\theta) ], \quad (3)$$

is a block-diagonal representation of the SO(2) action and  $R(k\theta)$  is the  $[2 \times 2]$  rotation matrix acting on the  $k$ -th Fourier mode. Lie algebra element  $T$  that generates (3) is also block-diagonal with  $[2 \times 2]$  generators of infinitesimal rotations  $T_k$  along its diagonal.  $R(k\theta)$  and  $T_k$  are explicitly written as follows:

$$R(k\theta) = \begin{pmatrix} \cos k\theta & -\sin k\theta \\ \sin k\theta & \cos k\theta \end{pmatrix}, \quad T_k = \begin{pmatrix} 0 & -k \\ k & 0 \end{pmatrix}. \quad (4)$$

Properties of Fourier modes can be stated compactly in the complex, U(1) formulation, but for visualization purposes we find it more convenient to work in the real SO(2)

representation. The group orbit  $\mathcal{M}_a$  of a state space point  $a$  is the set of all points reachable from  $a$  by symmetry transformations,  $\mathcal{M}_a = \{g(\theta)a \mid \theta \in [0, 2\pi)\}$ . In the method of slices, one constructs a ‘slice’, a submanifold  $\hat{\mathcal{M}} \subset \mathcal{M}$  that cuts each group orbit in an open neighborhood once and only once. The dynamics is then separated into the ‘shape-changing’ dynamics  $\hat{a}(\tau) \in \hat{\mathcal{M}}$  within this submanifold, and a transverse symmetry coordinate parameterized by the group parameter  $\theta(\tau)$  that reconstructs the original dynamics  $a(\tau) \in \mathcal{M}$  by the group action  $a(\tau) = g(\theta(\tau))\hat{a}(\tau)$ . For the  $\text{SO}(2)$  case at hand, a one-parameter set of transformations,  $\hat{\mathcal{M}}$  has one dimension less than  $\mathcal{M}$ .

There is a great deal of freedom in how one constructs a slice; in general one can pick any ‘moving frame’ [8–10]. Computationally easiest way to construct a local slice is by considering a hyperplane of points  $\hat{a}$  that satisfies

$$0 = \langle \hat{a} | t' \rangle, \quad \text{where} \quad \langle b | c \rangle = \sum_{k=1}^m b_k c_k. \quad (5)$$

Here,  $t'$  is the group tangent evaluated at a reference state space point  $\hat{a}'$  (or the ‘template’ [2]),  $t' = T\hat{a}'$ . The template is assumed not to lie in an invariant subspace, i.e.,  $g\hat{a}' \neq \hat{a}'$  for all  $g \neq 1$ . The dynamics within this slice hyperplane and the reconstruction equation for the phase parameter are given by

$$\begin{aligned} \hat{v}(\hat{a}) &= v(\hat{a}) - \dot{\theta}(\hat{a}) t(\hat{a}), \\ \dot{\theta}(\hat{a}) &= \langle v(\hat{a}) | t' \rangle / \langle t(\hat{a}) | t' \rangle, \end{aligned} \quad (6) \quad (7)$$

with  $t(\hat{a}) = T\hat{a}$  the group tangent evaluated at the symmetry-reduced state space point  $\hat{a}$ . Eq. (6) says that the full state space velocity  $v(\hat{a})$  is the sum of the in-slice velocity  $\hat{v}(\hat{a})$  and the transverse velocity  $\dot{\theta}(\hat{a}) t(\hat{a})$  along the group tangent, and (7) is the reconstruction equation whose integral tracks the trajectory in the full state space (for a derivation see, for example, ref. [11]).

The phase velocity (7) becomes singular for  $\hat{a}^*$  such that  $t(\hat{a}^*)$  lies in the slice,

$$\langle t(\hat{a}^*) | t' \rangle = 0, \quad (8)$$

or for  $\hat{a}^*$  in an invariant subspace, where  $t(\hat{a}^*) = 0$ . The  $(d-2)$ -dimensional hyperplane of such points  $\hat{a}^*$  forms the ‘slice border’, beyond which the slice does not apply. Both the slice hyperplane and its border depend on the choice of template  $\hat{a}'$ , with the resulting ‘chart’ in general valid only in some neighborhood of  $\hat{a}'$ . For a turbulent flow, symmetry reduction might require construction of a set of such local overlapping charts [6, 7]. However, as we now show for  $\text{SO}(2)$ , a simple choice of template may suffice to avoid all slice border singularities in regions of dynamical interest.

We define our ‘first Fourier mode slice’ by choosing a template that fixes the phase of the first Fourier mode,

$$\hat{a}' = (1, 0, 0, 0, \dots), \quad t' = (0, 1, 0, 0, \dots). \quad (9)$$

The slice determined by this template is the  $(d-1)$ -dimensional half-hyperplane

$$\begin{aligned} \hat{x}_1 &\geq 0, \quad \hat{y}_1 = 0, \\ \hat{x}_k, \hat{y}_k &\in \mathbb{R}, \quad \text{for all } k > 1. \end{aligned} \quad (10)$$

The condition  $\hat{y}_1 = 0$  follows from the slice condition (5), whereas  $\hat{x}_1 \geq 0$  ensures a single intersection for every group orbit. The denominator of (7) approaches zero as the trajectory approaches the slice border,  $\hat{x}_1(\tau) \rightarrow 0$ . This singularity can be regularized by defining the in-slice time as  $d\hat{\tau} = d\tau/\hat{x}_1$ , and rewriting (6) and (7) as

$$d\hat{a}/d\hat{\tau} = \hat{x}_1 v(\hat{a}) - \hat{y}_1(\hat{a}) t(\hat{a}), \quad (11)$$

$$d\theta(\hat{a})/d\hat{\tau} = \hat{y}_1(\hat{a}). \quad (12)$$

The phase velocity (12) is now the non-singular, full state space velocity component  $\hat{y}_1$  orthogonal to the slice, and the full state space time is the integral

$$\tau(\hat{\tau}) = \int_0^{\hat{\tau}} d\hat{\tau}' \hat{x}_1(\hat{\tau}'). \quad (13)$$

For example, the full state space period  $\tau_p = \tau_p(\hat{\tau}_p)$  of a relative periodic orbit  $a(\tau_p) = g_p a(0)$  is the integral (13) over one period  $\hat{\tau}_p$  in the slice.

We illustrate this symmetry reduction scheme by two examples. For clarity, we first apply the method to a model with only two coupled Fourier modes, and then apply it to the Kuramoto-Sivashinsky equation on a one-dimensional periodic domain.

‘Two-mode system’ is a two-Fourier modes system studied in ref. [12–15] as normal form close to bifurcations off an  $\text{SO}(2)$  invariant equilibrium. Our two-mode ODEs are [16]:

$$\begin{aligned} \dot{x}_1 &= (\mu_1 - r^2)x_1 + c_1(x_1x_2 + y_1y_2), \quad r^2 = x_1^2 + y_1^2 \\ \dot{y}_1 &= (\mu_1 - r^2)y_1 + c_1(x_1y_2 - x_2y_1) \\ \dot{x}_2 &= x_2 + y_2 + x_1^2 - y_1^2 + a_2x_2r^2 \\ \dot{y}_2 &= -x_2 + y_2 + 2x_1y_1 + a_2y_2r^2, \end{aligned} \quad (14)$$

with parameter values  $\mu_1 = -2.8$ ,  $a_2 = -2.66$ ,  $c_1 = -7.75$  empirically chosen so the system exhibits chaos. The flow satisfies the  $\text{SO}(2)$  equivariance condition (2) by construction, with the Lie group element (3) truncated at the second mode. Furthermore,  $r = 0$  is a flow-invariant subspace. That guarantees that in-slice trajectories can only approach the slice border  $\hat{x}_1 = 0$ , but never cross it; hence the symmetry-reduced dynamics is confined to the slice half-hyperplane for all times.

Fig. 1(a) shows the only relative equilibrium of the two-mode system, a typical chaotic orbit, and its shortest relative periodic orbit projected down to 3 dimensions from the 4D state space. In the full state space the group orbit of a relative periodic orbit is a torus, traced out ergodically by repeats of the relative periodic orbit.

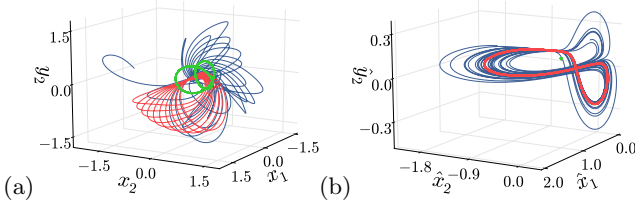


FIG. 1: (Color online) The two-mode system: A typical chaotic trajectory (blue), a trajectory spiraling out from the relative equilibrium (green), 10 repeats of the shortest  $\tau_p = 3.6415120$  relative periodic orbit (orange) plotted in (a) a 3D projection of its four-dimensional state space; (b) the three-dimensional slice hyperplane.

Fig. 1 (b) illustrates why symmetry-reduction is absolute prerequisite to any analysis of the topology of a strange attractor. Here, the same flow is shown in the three-dimensional symmetry-reduced slice hyperplane. The full state space relative equilibrium is reduced to an equilibrium and the relative periodic orbit to a periodic orbit. Once the drifts along the symmetry direction have been quotiented out, a chaotic attractor, shaped by the relative equilibrium and the equilibrium at the origin, is revealed [16].

#### Kuramoto-Sivashinsky system

$$u_t = -\frac{1}{2}(u^2)_x - u_{xx} - u_{xxx}$$

in a periodic domain has been extensively studied as a model PDE exhibiting spatiotemporal chaos. The relative equilibrium and relative periodic orbit solutions that we use in this example are described in ref. [17], where the domain size has been set to  $L = 22$ , large enough to exhibit complex spatiotemporal dynamics. In terms of complex Fourier modes (1) the Kuramoto-Sivashinsky equation is:

$$\dot{\tilde{u}}_k = (q_k^2 - q_k^4) \tilde{u}_k - i \frac{q_k}{2} \sum_{m=-\infty}^{+\infty} \tilde{u}_m \tilde{u}_{k-m}, \quad (15)$$

where  $q_k = 2\pi k/L$ . Expressed in the real  $SO(2)$  representation  $\tilde{u}_k = x_k + i y_k$ , Kuramoto-Sivashinsky equation is equivariant under  $SO(2)$  rotations (3). We have adapted the ETDRK4 method [18, 19] for numerical integration of the symmetry reduced equations (11), where we set  $\tilde{u}_0 = 0$  and truncate the expansion (15) to  $m = 15$  Fourier modes, so the state space is 30-dimensional,  $a = (x_1, y_1, x_2, y_2, \dots, x_{15}, y_{15})^T$ .

As an illustration of symmetry reduction, we trace out a segment of the unstable manifold of the relative equilibrium (travelling wave)  $TW_{-1}$  by integrating  $k$  trajectories with initial conditions  $\hat{a}_1, \dots, \hat{a}_k$ ,

$$\hat{a}_\ell = \hat{a}_{TW_{-1}} + \epsilon e^{i\ell\delta} \hat{e}_1, \quad \text{where } \delta = 2\pi\mu^{(1)}/k\omega^{(1)}. \quad (16)$$

Here  $\hat{a}_{TW_{-1}}$  is the point of intersection of the  $TW_{-1}$  orbit with the slice hyperplane,  $\epsilon$  is a small parameter

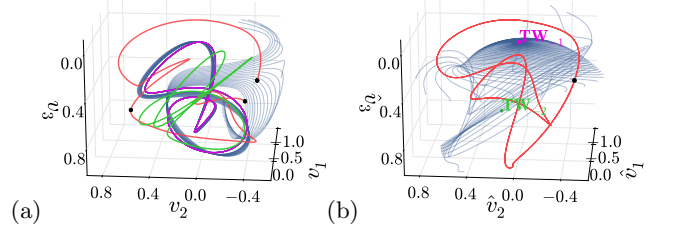


FIG. 2: (Color online) Kuramoto-Sivashinsky system: (a) Unstable manifold of the relative equilibrium  $TW_{-1}$  (blue) computed by integrating 20 nearby points given by (16) for  $\tau = 120$ ; 2 repeats of the  $\tau_p = 33.5010$  relative periodic orbit (red), with instants  $\tau = 0, \tau_p, 2\tau_p$  marked by black dots; group orbits (which are also the time orbits) of the  $TW_{-1}$  (magenta) and  $TW_{-2}$  (green) in the full state space. The coordinate axes are projections ( $v_1, v_2, v_3$ ) onto three orthonormal vectors ( $\hat{e}_1, \hat{e}_2, \hat{e}_3$ ), respectively, constructed from  $\text{Re } \hat{V}_1$ ,  $\text{Im } \hat{V}_1$  and  $\text{Re } \hat{V}_2$  via Gram-Schmidt orthogonalization.  $\hat{V}_1$  and  $\hat{V}_2$  are the first and second most expanding complex stability eigenvectors of  $TW_{-1}$ . (b) The same solutions in the slice hyperplane.  $TW_{-1}$  and  $TW_{-2}$  solutions have now collapsed into single points, the unstable manifold is a smooth 2D surface, and the relative periodic orbit closes after a single period.

that we set to  $10^{-6}$  and  $\hat{e}_1 = \text{Re } \hat{V}_1 / |\text{Re } \hat{V}_1|$ . The unstable manifold of  $TW_{-1}$  is four-dimensional: here we present the two-dimensional submanifold associated with the most expanding complex linear stability eigenvector  $\hat{V}_1$  of  $TW_{-1}$ , with the eigenvalue  $\lambda^{(1)} = \mu^{(1)} + i\omega^{(1)}$ . Fig. 2 shows the state space projections of unstable manifold of  $TW_{-1}$  along with the  $\tau_p = 33.5010$  relative periodic orbit and the relative equilibrium  $TW_{-2}$ . It is clear from fig. 2(a) that without the symmetry reduction, the  $TW_{-1}$  unstable manifold is dominated by the drifts along its group orbit. In the symmetry reduced state space  $\hat{\mathcal{M}}$ , shown in fig. 2(b), the dynamically important, group-action transverse part of the unstable manifold of  $TW_{-1}$  is revealed. While the drifts along the symmetry direction complicate the relative periodic orbit in fig. 2(a), the same orbit closes onto itself after one repeat within the slice hyperplane, fig. 2(b). Likewise,  $TW_{-2}$ , which is topologically a circle but appears convoluted in the projection of fig. 2(a), is reduced to a single equilibrium point. The stage is now set for a construction of symbolic dynamics for the flow by means of Poincaré sections and Poincaré return maps [20].

The solutions of Kuramoto-Sivashinsky system are conventionally visualized in the configuration space, as time evolution of color-coded value of the function  $u(x, t)$ , see fig. 3. Fig. 3(b) and (e) illustrate that a relative equilibrium and a relative periodic orbit become an equilibrium and a periodic orbit after symmetry reduction. Fig. 3(b) shows that even after the numerical trajectory diverges from the unstable relative equilibrium and falls onto the strange attractor, our symmetry reduced representation stays valid. The sharp shifts (along  $x$  direction)

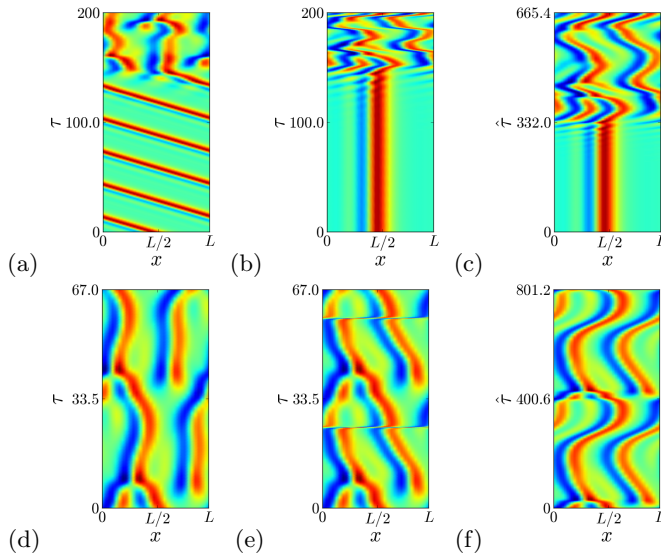


FIG. 3: (Color online) Traveling wave  $TW_{-1}$  with phase velocity  $c = 0.737$  in configuration space: (a) the full state space solution, (b) symmetry-reduced solution with respect to the lab time, and (c) symmetry-reduced solution with respect to the in-slice time. Relative periodic orbit  $\tau_p = 33.50$  in configuration space: (d) the full state space solution, (e) symmetry-reduced solution with respect to the lab time, and (f) symmetry-reduced solution with respect to the in-slice time.

in fig. 3(e) correspond to the time intervals where trajectory has a nearly vanishing first Fourier mode. Plotted as the function of the in-slice time  $\hat{\tau}$  in fig. 3(f), these rapid episodes are well resolved.

Unlike the two-mode example, the slice border for Kuramoto-Sivashinsky is not a flow-invariant subspace and is not protected from a trajectory visit. However, our numerical simulations of long-time ergodic trajectories have not actually encountered this passage (the case of solutions in invariant subspaces requires some care and will be treated elsewhere [20]). Thus, for the Kuramoto-Sivashinsky (and Navier-Stokes [21]) cases our argument is probabilistic: the likelihood that a generic turbulent state has exactly (to the machine precision, for computer simulations) vanishing first Fourier mode,  $\tilde{u}_1 = 0$ , is small. Note that  $x_1 = y_1 = 0$  is a stagnation subspace of the rescaled time evolution (11). It would take a trajectory an infinitely long time (in the in-slice time  $\hat{\tau}$  units) to reach this subspace, which is why integrating (11) resolves close passages to the border very well.

In summary, we recommend that the ‘first Fourier mode slice’ (9), a simple  $SO(2)$  symmetry reduction prescription, be used to reduce the  $SO(2)$  symmetry of spatially extended systems. This slice is valid as long as the amplitude of the first Fourier mode is non-zero. Small periodic cell Kuramoto-Sivashinsky and Navier-Stokes simulations indicate that the first mode can approach zero, but never completely vanishes. Regularizing the sym-

metry reduced velocities (6) and (7) by a time-scaling transformation resolves the reduced flow well in these instances.

Our examples demonstrate that the symmetry reduced flows are considerably simpler and provide enhanced understanding of the global organization of different solutions and their invariant manifolds. A technically more demanding demonstration of the validity of our method for a Navier-Stokes flow is described in ref. [21].

We are indebted to Xiong Ding and Francesco Fedele for stimulating discussions and to Daniel Borrero-Echeverry for a critical reading of the manuscript. Matplotlib library [22] was used to produce the figures in this letter.

- 
- [1] B. Hof, C. W. H. van Doorne, J. Westerweel, F. T. M. Nieuwstadt, H. Faisst, B. Eckhardt, H. Wedin, R. R. Kerswell, and F. Waleffe, *Science* **305**, 1594 (2004).
  - [2] C. W. Rowley and J. E. Marsden, *Physica D* **142**, 1 (2000).
  - [3] W.-J. Beyn and V. Thümmel, *SIAM J. Appl. Dyn. Syst.* **3**, 85 (2004).
  - [4] E. Siminos and P. Cvitanović, *Physica D* **240**, 187 (2011).
  - [5] S. Froehlich and P. Cvitanović, *Commun. Nonlinear Sci. Numer. Simul.* **17**, 2074 (2012), [arXiv:1101.3037](#).
  - [6] P. Cvitanović, D. Borrero-Echeverry, K. Carroll, B. Robbins, and E. Siminos, *Chaos* **22**, 047506 (2012).
  - [7] A. P. Willis, P. Cvitanović, and M. Avila, *J. Fluid Mech.* **721**, 514 (2013), [arXiv:1203.3701](#).
  - [8] E. Cartan, *La méthode du repère mobile, la théorie des groupes continus, et les espaces généralisés*, vol. 5 of *Exposés de Géométrie* (Hermann, Paris, 1935).
  - [9] M. Fels and P. J. Olver, *Acta Appl. Math.* **51**, 161 (1998).
  - [10] E. L. Mansfield, *A practical guide to the invariant calculus* (Cambridge Univ. Press, Cambridge, 2010).
  - [11] P. Cvitanović, R. Artuso, R. Mainieri, G. Tanner, and G. Vattay, *Chaos: Classical and Quantum* (Niels Bohr Inst., Copenhagen, 2014), [ChaosBook.org](#).
  - [12] G. Dangelmayr, *Dyn. Sys.* **1**, 159 (1986).
  - [13] C. A. Jones and M. R. E. Proctor, *Phys. Lett. A* **121**, 224 (1987).
  - [14] M. Golubitsky, I. Stewart, and D. G. Schaeffer, *Singularities and Groups in Bifurcation Theory, vol. II* (Springer, New York, 1988).
  - [15] J. Porter and E. Knobloch, *Physica D* **201**, 318 (2005).
  - [16] N. B. Budanur, D. Borrero-Echeverry, P. Cvitanović, and E. Siminos (2014), in preparation.
  - [17] P. Cvitanović, R. L. Davidchack, and E. Siminos, *SIAM J. Appl. Dyn. Syst.* **9**, 1 (2010), [arXiv:0709.2944](#).
  - [18] S. M. Cox and P. C. Matthews, *J. Comput. Phys.* **176**, 430 (2002).
  - [19] A.-K. Kassam and L. N. Trefethen, *SIAM J. Sci. Comput.* **26**, 1214 (2005).
  - [20] E. Siminos, N. B. Budanur, P. Cvitanović, and R. L. Davidchack (2014), in preparation.
  - [21] A. P. Willis, K. Y. Short, and P. Cvitanović (2014), in preparation.
  - [22] J. D. Hunter, *Comput. Sci. Eng.* **9**, 90 (2007).